532.582

Paper No. 188-7

Characteristics of the Flow around Two Circular Cylinders Arranged in Tandem * (1st Report)

By Tamotsu IGARASHI **

Experimental investigations on the characteristics of the flow around two circular cylinders in a cross flow were carried out. Reynolds number was varied in the range of subcritical values, $8.7\times10^3 \leqq Re \leqq 5.2\times10^4$ and the distance between the axes of the cylinders in the spacings $1.03 \leqq L/d \leqq 5.0$, where d is the diameter of the cylinder.

Up to the spacings of $L/d = 3.5$, where the quasi-stationary vortices are formed between the cylinders, the changes of the flow structure around the two cylinders were observed at the spacings of $L/d = 1.1$, 1.6, 2.3 and 3.1. Particularly, the dependency of the Reynolds number was recognized in the range of $1.1 \leqq L/d \leqq 2.0$.

1. Introduction

In a flow across tube banks of a heat exchanger for instance, oscillation and heat transfer of tubes become important problems. In the fields of civil engineering and architecture, aerodynamic characteristics of a body in the wake of another bluff body arouse interest in connection with the wind effects on the plural chimneys and skyscrapers in recent years. Pressure drop and heat transfer across banks of pipes in the heat exchangers[1] have been investigated for a long time. Recently it has become a serious problem that the vibration, noise and unsteady fluid forces on the tube-bank heat-exchangers which tend to increase in size and flow speed, are induced by the von Karman vortex streets. From the above viewpoint, Ishigai, et al.[2],[3] investigated the structure of gas flow in tube banks with various arrangements. Chen[4] and Tokushima[5] investigated on the problem of vibration, noise and pressure fluctuation in tube-bank heat-exchangers. A simple experimental model of tube banks with two circular cylinders in a cross flow (one of them being in the wake of the other) has been investigated by many workers. Studies on steady and unsteady fluid forces acting on two cylinders in tandem arrangement and on the vortex shedding frequency behind the cylinders were started by Biermann and Herrenstein[6] and then followed by Hori[7], Suzuki, et al.[8], Watanabe, et al.[9], Imaichi, et al.[10] and Tokushima, et al.[11]. Experimental studies on fluid flow and heat transfer around two cylinders have been carried out by Kostic and Oka[12] and Hiwada, et al.[13]. These investigations were carried out in subcritical Reynolds number range. Recently Okajima[14] made an experiment in supercritical Reynolds number range. The flow patterns around two cylinders can be divided into two types at a value of about 3.5 to 3.8 in the spacing between the axes of two cylinders, L/d. It is well known that the drag coefficient acting on two cylinders and the Strouhal number of the vortex shedding make discontinuous changes at the critical spacing. In this paper, this discontinuous change is called a jump phenomenon.

The flow around two cylinders in tandem arrangement, however, has not been clarified completely, and there still remain a number of unclarified points concerned. Comparing previous investigations, many disagreements between them are perceived. Concerning the variation of the flow patterns around the cylinders for the spacing up to $L/d = 3.5$, Imaichi, et al.[10] and Tokushima, et al.[11] pointed out that the flow is unstable in the range of the spacings $1.5 \leqq L/d \leqq 1.8$, and at a spacing of $L/d = 1.2$ the concentration of the vortices in the wake of the downstream cylinder is remarkably decreased, so that there exists no distinct frequency component. On the other hand, Hiwada, et al.[13] stated in their report that the flow in a closed vortex changed from quasi-stationary flow to intermittent periodic flow at a spacing of $L/d = 2.5$. Regarding the position of the reattachment of the shear layer from the upstream cylinder onto the downstream cylinder, Kostic and Oka[12] wrote that the reattachment position move forward as the spacing increased beyond $L/d = 2.5$. Hiwada, et al.[13], contrary to the above, indicated that the reattachment position move back at first and then the location did not move up to the critical spacing. Hori[7] presented that the Strouhal number and the base pressure of the cylinders depended on the Reynolds number and its effect was very complicated. On the other hand, Ishigai, et al.[3] reported that the Reynolds number effect could be neglected. The author[15] reported that the changes of the flow structure around two cylinders were observed at the spacings of $L/d = 1.1$ and 2.0, and the Strouhal number varied remarkably with the free stream velocity in the range of the spacings $1.1 \leqq L/d \leqq 2.0$. Recently Zdravkovich[16] reviewed a number of investigations in the field.

* Received 2nd April, 1979.
** Associate Professor,
The National Defence Academy
1-10-20 Hashirimizu, Yokosuka.

NII-Electronic Library Service

From the viewpoint aforementioned, a detailed experimental investigation in connection with an unsteady flow around two circular cylinders arranged in tandem was carried out.

Nomenclature

C_D : drag coefficient = $\int_0^{\pi} C_p \cos\phi \, d\phi$
C_p : pressure coefficient = $(p-p_o)/0.5\rho u_o^2$
d : diameter of circular cylinder
f : vortex shedding frequency or frequency
L : longitudinal spacing between the axes of the cylinders
p_o : static pressure at free stream
p : pressure or time-averaged pressure
p' : fluctuation pressure
Re : Reynolds number = $u_o d/\nu$
S : Strouhal number = fd/u_o
u_o : free stream velocity
x : streamwise coordinate from the center of downstream cylinder
y : coordinate perpendicular to x
ν : kinematic viscosity of fluid
ρ : density of fluid
ϕ : circumferential angle on the cylinder

Subscripts
1,2 : upstream and downstream cylinders

2. Experimental apparatus and procedure

The configuration of the two cylinders is shown in Fig. 1. The upstream and downstream cylinders arranged in an uniform flow having its width H, are denoted by the subscripts 1 and 2 respectively. Let L be the longitudinal spacing between the centers of the cylinders and ϕ the angle on the circumference taken from the front stagnation point on each cylinder. Let x, y be the streamwise and normal coordinates measured from the center of the downstream cylinder. Both cylinders were d = 34 mm in diameter and the free stream velocity u_o varied from 4 m/s to 24 m/s. The Reynolds numbers were in the range of $8.7\times10^3 \leqq Re \leqq 5.2\times10^4$. Tests were carried out in a wind tunnel whose test section was 600 mm × 150 mm (H = 600 mm). The effects of the spacings ($1.03 \leqq L/d \leqq 5.0$) and the Reynolds number on the flow characteristics were investigated. Flow visualizations were performed by a smoke wind tunnel and an oil-film method at the velocity u_o = 6 and 16 m/s respectively. The pressure distributions around the cylinders were measured by a manometer, rotating the cylinder having pressure taps of 0.6 and 1.0 mm diameter, in the range of u_o = 6 ~ 20 m/s. And pressure fluctuations were measured by a semi-conductor pressure converter connected with the pressure tap in the range of u_o = 10 ~ 20 m/s. Velocity fluctuations in the wake of the cylinders were measured by an anemometer in a wind tunnel whose test section was 400 mm × 150 mm (H = 400 mm). A frequency analysis of its fluctuations was performed. The Strouhal number of the vortex shedding from the cylinders was obtained from the above analysis in the range of u_o = 4 ~ 24 m/s.

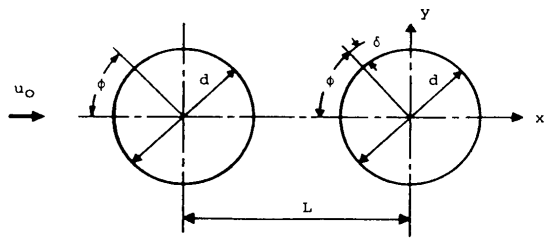

Fig.1 Coordinate system and symbols

3. Experimental results

3.1 Pressure distribution and drag coefficinet

The pressure coefficient distributions around the two cylinders at $Re = 3.5\times10^4$ are shown in Fig.2 for five different spacings. The pressure distribution around the upstream cylinder shows a laminar separation. For small spacings up to 3.5 dia., the rear parts of the curve show flat pressure dis-

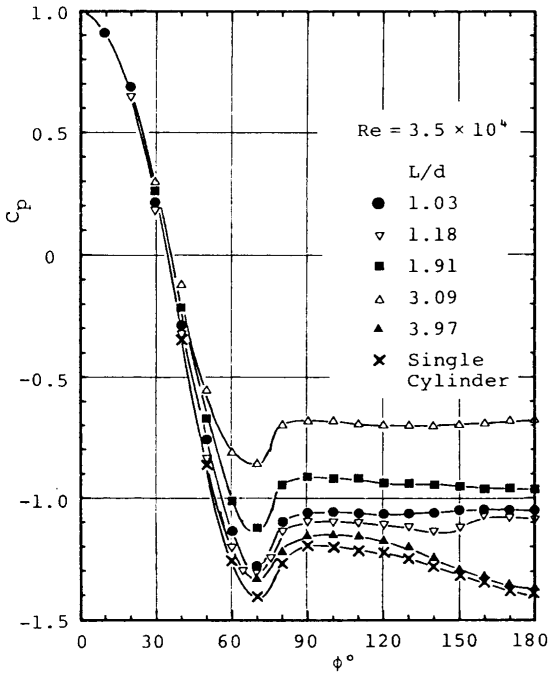

(a) upstream cylinder

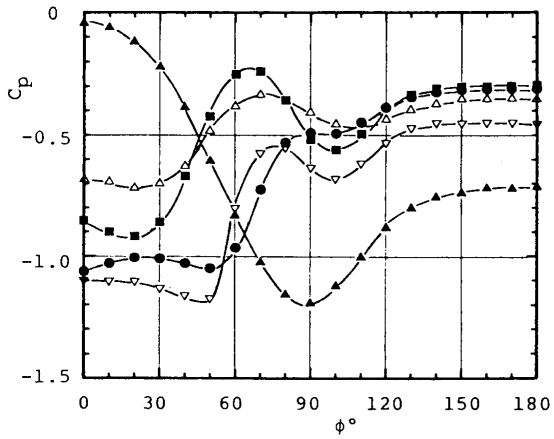

(b) downstream cylinder

Fig. 2 Pressure distribution around two cylinders

NII-Electronic Library Service

tributions and the base pressure coefficients are almost the same as the pressure coefficients of the front stagnation point of the downstream cylinder. This fact indicates quasi-stationary vortices being formed in the gap between the cylinders. The base pressure coefficient of the upstream cylinder increases as the spacing increases. Because the separated shear layer from the upstream cylinder rolls up in front of the downstream cylinder, the pressure distribution for $L/d = 3.97$ presents a similar curve to the one for a single cylinder. Up to the critical spacing of $L/d = 3.5$, the pressure distribution around the downstream cylinder shows a very low negative pressure near the front stagnation point and a maximum value at the position of the reattachment point of the separated shear layer from the upstream cylinder. The reattachment point is located at around $\phi = 70°$, although a small shift of the reattachment point can be seen depending on Reynolds number and the spacing. For the spacing of about 2.35 dia. the reattachment point moves up to the position at $\phi = 60°$. At the spacing of 1.03 dia., there is no sign of the reattachment peak. This fact indicates that the separated shear layer from the upstream cylinder does not reattach onto the downstream cylinder. The base pressure of the downstream cylinder increases remarkably a value between -0.3 and -0.5. Beyond the spacing of 3.5 dia., the curve has a maximum value at the stagnation point and shows a similar distribution to that of the single cylinder with turbulent separation. Examining the variation of the pressure coefficient around the downstream cylinder against the spacing in detail, one can see that the pressure coefficient does not decrease monotonously. The pressure coefficient on the front surface has a large negative value in the range of spacings $1.03 \leqq L/d \leqq 1.91$, which has the minimum value at $L/d = 1.32$ and increases as the spacing increases beyond that spacing. With an increase in the spacings above $L/d = 2.09$, the pressure coefficient starts to decrease. But it increases again beyond $L/d = 2.35$. The variation of the base pressure coefficient corresponds to the variation of the pressure coefficient at the front stagnation point. As mentioned above, the change of the flow structure around the cylinders takes place at the spacific spacings in the case of the formation of a quasi-stationary vortex between the cylinders.

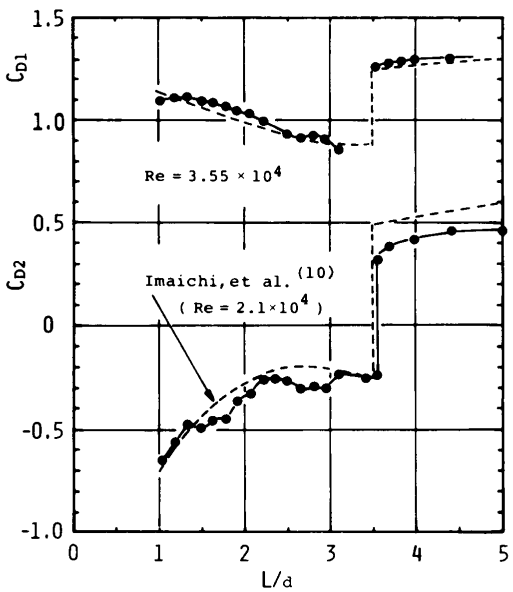

Fig. 3 Drag coefficient of two cylinders

The drag coefficients obtained by integration of the pressure distribution are shown together with the result of Imaichi, et al.[10] in Fig. 3. The drag coefficients of the upstream cylinder, C_{D1}, decrease gradually in inverse proportion to the spacing of two cylinders corresponding to the change of the base pressure coefficient. At spacings of about 3.53 to 3.68 dia., the drag coefficient increases stepwise and then approaches 1.30. This value becomes 1.17 with a correction for the blockage effects, and agrees with that of the single cylinder. This critical spacing agrees well with the critical spacing from 3.5 to 3.8 dia. in the previous reports[10]~[14] for subcritical Reynolds number region. On the other hand, the drag coefficient of the downstream cylinder, C_{D2}, is minus, so that the drag force acts as a thrust. The thrust has a maximum value of 0.65 at the minimum spacing, and continues to decrease as the spacing increases. This drag coefficient shows a peak near the spacing of $L/d = 2.5$, which is also true in the previous reports[6],[13]. Beyond the critical spacing, the drag coefficient changes from negative to positive and the magnitude is nearly constant at a value of 0.45.

3.2 Strouhal number

Vortex shedding frequencies behind the downstream cylinder are obtained by a frequency analysis of the velocity fluctuation at $x = 2d$ and $y = 0.5d$. The results for two Reynolds numbers are shown in Fig. 4. At small gap of $L/d = 1.03$, two cylinders work just as a single body connected by the stagnant region in the gap. Therefore the Strouhal number ($S = 0.27$) is nearly the

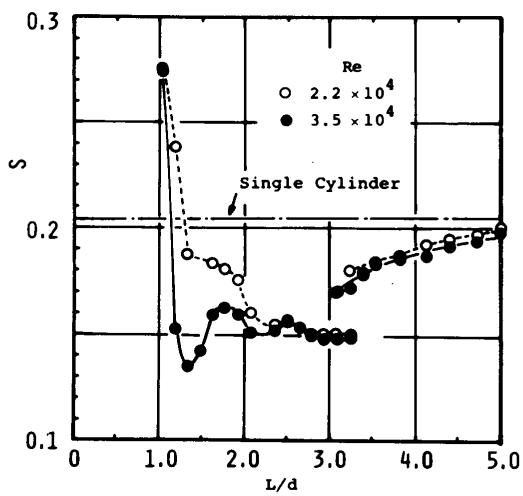

Fig. 4 Strouhal number behind downstream cylinder

NII-Electronic Library Service

same as that of a slender body. In the range of $1.18 \leqq L/d \leqq 2.06$, the Strouhal number depends very strongly on Reynolds number. In particular, the flow is irregular and unstable at $Re = 2.2\times10^4$ ($u_0 = 10$ m/s), as shown in Fig. 11(a). In the range of $2.06 \leqq L/d \leqq 2.94$, the effect of Reynolds number on the Strouhal number is not remarkable. And the most regular vortex streets are formed behind the downstream cylinder for the spacings from 2.35 to 2.5 diameter. Up to the critical spacing the Strouhal number is nearly constant, $S = 0.15$. In the range of the spacings $3.09 \leqq L/d \leqq 3.53$, two different values of Strouhal number exist because of the vortex shedding from the upstream cylinder and an intermittent jump phenomenon. Hiwada, et al.[13] obtained the same results. Beyond the critical spacing 3.53 dia., the Strouhal number increases as the spacing increases and approaches the value found behind the single cylinder. Figure 5 shows the effect of Reynolds number on Strouhal number. In the range of the spacing $1.18 \leqq L/d \leqq 2.06$, the Strouhal number decreases remarkably as Reynolds number increases. Therefore, it is clear that the flow pattern around two cylinders changes depending on Reynolds number in this range of the spacings. For the spacing of $L/d = 1.03$ and above $L/d = 2.06$, the Strouhal number is almost constant in the range of Reynolds numbers $1.7\times10^4 \leqq Re \leqq 5.2\times10^4$. It is considered that there is no change of the flow pattern depending on Reynolds number in those spacings.

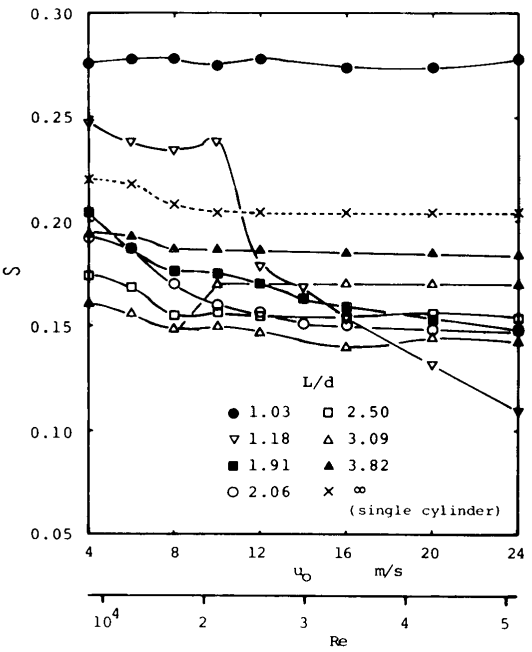

Fig. 5 Effects of Reynolds number on Strouhal number

3.3 Flow visualization

A typical flow visualization using a smoke wind tunnel at $Re = 1.3\times10^4$ is shown in Fig. 6. At the spacing of $L/d = 1.03$, the flow looks like that of a single body. In the range of the spacings $1.18 \leqq L/d \leqq 1.91$, the separated shear layers develop rather straight without reattaching onto the downstream cylinder and the width of the wake is considerably reduced comparing with that of a single cylinder. The vortex formation region is shifted downstream as the spacing increases. At the spacings $L/d = 2.06$ and 3.09, the separated shear layer is reattached onto the downstream cylinder. The vortex formation region approaches rapidly the downstream cylinder and the vortices are shed at regular intervals. The flow at the spacing of $L/d = 3.97$ is a jumped flow. The near wake of the upstream cylinder is similar to that of the single cylinder without interference of the downstream cylinder. On the other hand, the downstream cylinder in a periodic alternative shear flow presents a complicated flow field. Up to the spacings of $L/d = 1.91$, the separated shear layer from the upstream cylinder does not reattach onto the downstream cylinder as shown in Fig. 6. But the pressure distribution for $Re = 3.5\times10^4$ shows a reattachment of the shear layer as is obvious from Fig. 2. Then, the flows on the two cylinders were visualized by an oil-film method at the same Reynolds number for the pressure distribution. The results are shown in Fig. 7. Reattachment line on the downstream cylinder appears at a position which presents the maximum value of the pressure coefficient. The separated lines at both sides of the reattachment line are shown near the positions which present the minimum value of the pressure coefficient respectively. Difference between Figs. 6 and 7 indicates that the flow pattern changes depending on Reynolds number corresponding to the effect of Reynolds number on Strouhal number as shown in Fig. 5.

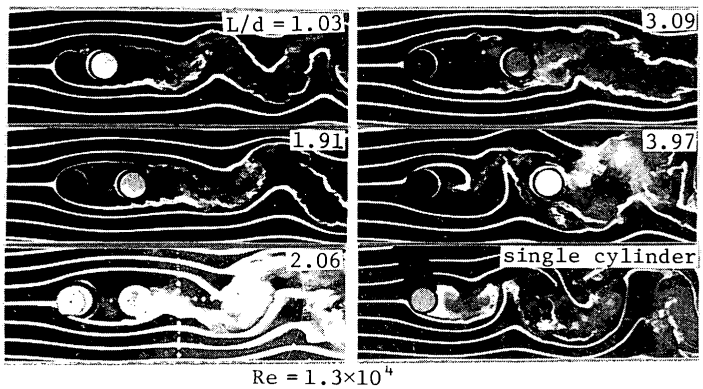

$Re = 1.3\times10^4$

Fig. 6 Flow visualization by smoke wind tunnel

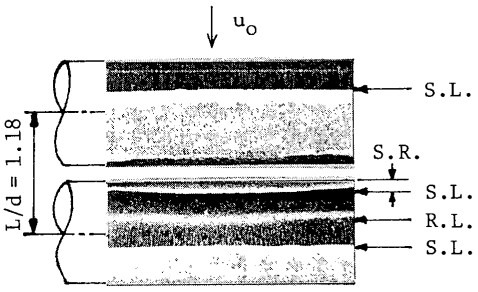

$Re = 3.5\times10^4$

R.L. : Reattachment line
S.L. : Separation line
S.R. : Separation region

Fig. 7 Surface oil-flow patterns on two cylinders

NII-Electronic Library Service

3.4 Pressure fluctuation

In order to make clear the fluid flow around two cylinders, the distributions of R.M.S. (root mean square) pressure fluctuations on the surface of the cylinders were measured. Figure 8 (a) and (b) show the results at $Re = 3.5\times10^4$. The R.M.S. profiles on the upstream cylinder have peak values near the separation point. Up to the critical spacing the R.M.S. values are remarkably small. Beyond the critical spacing, the profile is similar to, but slightly larger than, that of the single cylinder. And further, there is a second peak on the rear surface about $\phi = 160°$. This is due to the shear layer rolling up and forming a large separated vortex, while the reverse flow reattaches on the rear surface and then again separates at the second peak position. Examining in detail the variation of the R.M.S. profiles, it is seen that the pressure fluctuations near the spacings of $L/d = 1.32$ and 2.5 are large and correspond to the distribution of the time-averaged pressure coefficients as shown in Fig. 2 . The variation of R.M.S. values correspond exactly to that of the pressure coefficients at $\phi = 0°$ of the downstream cylinder rather than to that of the base pressure coefficients of the upstream cylinder. The pressure fluctuation around the downstream cylinder is very large. The magnitude of the R.M.S. value is in proportion to that for the upstream cylinder and to the time-averaged pressure coefficient at $\phi = 0°$ of the downstream cylinder. Up to the critical spacing, it is seen that these variations which depend on the spacing are due to the behavior of the reattachment of the separated shear layer from the upstream cylinder. The profiles of the R.M.S. value have two peaks. The position of the first peak comes slightly in front of the reattachment point and the second peak is at the separation point on the rear surface of the cylinder. For the spacings of $1.18 \leqq L/d \leqq 1.91$, the second peak is higher than the first peak. Particularly a third peak appears at the separation point on the front surface of the cylinder in the range of $1.18 \leqq L/d \leqq 1.47$. For the spacings of $2.06 \leqq L/d \leqq 3.09$, the first peak is higher than the second peak. The R.M.S. value near the front stagnation point ($\phi = 0°$) of the downstream cylinder is considerably higher than that of the rear stagnation point ($\phi = 180°$) of the upstream cylinder. comparing the value of the front surface of the downstream cylinder for $L/d < 2.0$ with that for $L/d \geqq 2.0$, it is obvious that the fluid flow between two cylinders for the spacings of $L/d = 2.0$ is more active than that for $L/d < 2.0$. And the two peaks at the spacings of $L/d = 2.35$ and 2.50 are higher than that of the other spacings. In the range of the spacings $3.09 \leqq L/d \leqq 3.53$, the second peak is nearly flat. At $L/d = 3.83$ beyond the critical spacing, the R.M.S. values marked out by the scale on the right side of the figure, are very large. The profiles have two peaks. One of them is near the turbulent separation point at $\phi = 110°$, which is moderate and disappears as the spacing increases. The other is a sharp peak at $\phi = 40°$, its location and magnitude are remain unchanged up to the spacing of $L/d = 7.0$. Figure 9 shows the distribution of the R.M.S. pressure fluctuations around the downstream cylinder for $L/d = 1.18$. At this spacing there is a remarkable effect of Reynolds number on the flow patterns (see Fig. 5). The second peak does not

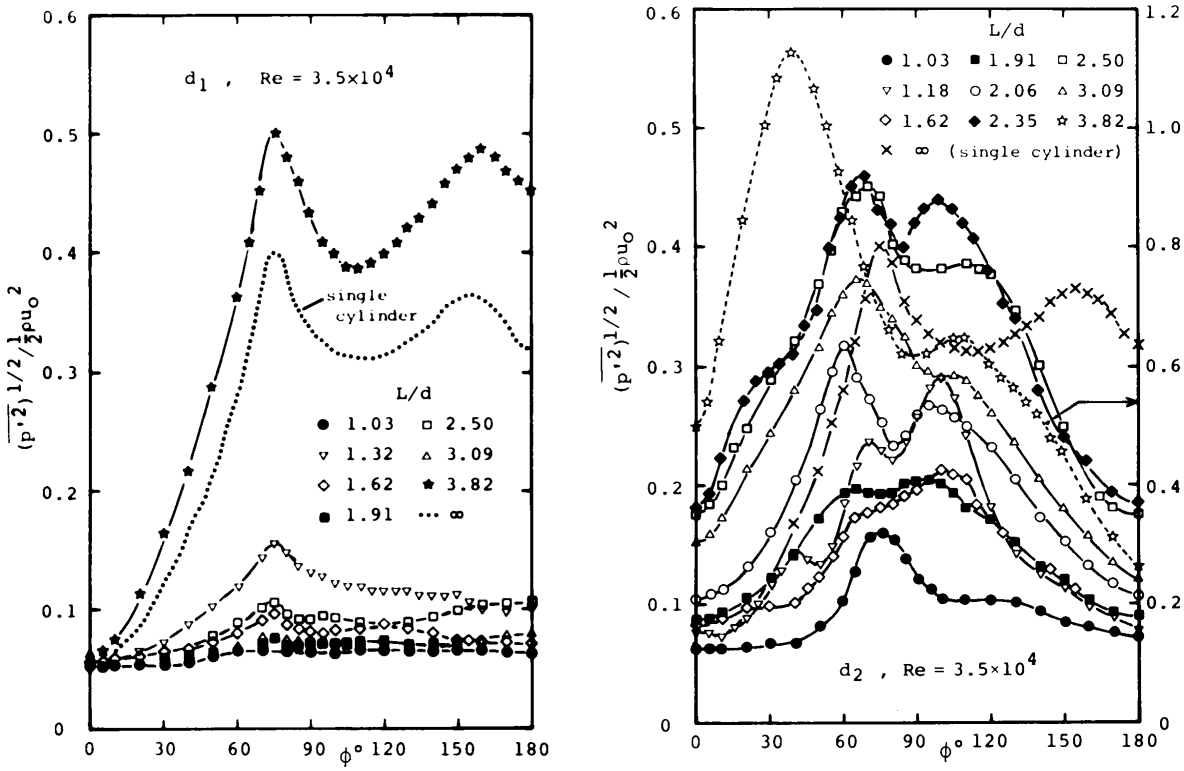

(a) upstream cylinder (b) downstream cylinder

Fig. 8 Distribution of R.M.S. pressure fluctuation around two cylinders

NII-Electronic Library Service

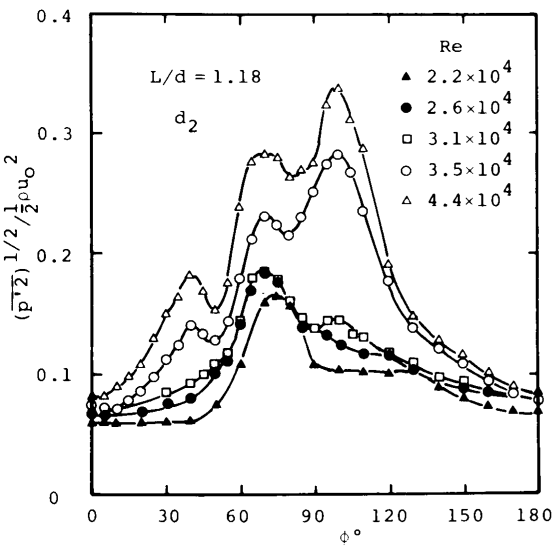

Fig. 9 Distributions of R.M.S. pressure fluctuation around downstream cylinder

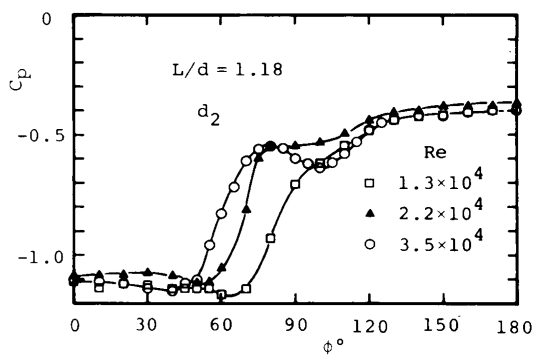

Fig. 10 Pressure distribution around downstream cylinder

appear for Re ≦ 2.6×10⁴ and appears at Re = 3.1×10⁴. The second peak is considerably lower than the first peak. For Re ≧ 3.5×10⁴, the third peak appears and the second peak becomes higher than the first peak. The Reynolds number effects were investigated for other spacings. The effect is most prominent in the range of the spacings 1.18 ≦ L/d ≦ 1.47 and remarkably less so in the range of 1.62 ≦ L/d ≦ 1.91. The effect does not appear for L/d = 1.03 and L/d ≧ 2.06, when the profiles of the R.M.S. values for Re ≧ 2.2×10⁴ are similar to those in Fig. 8 (b).

4. Discussion

In the previous chapters, for the spacings up to L/d = 3.5, it is shown that the structure of the flow around the cylinders is divided into five categories at the spacings of L/d = 1.03, 1.62, 2.35 and 3.09. Particularly, the dependency of Reynolds number on the flow pattern is also found in the range of the spacings 1.03 ≦ L/d ≦ 2.0. In this chapter, we discuss the structure of those patterns and classify the patterns in detail, to clarify those characteristics of the flow around two cylinders.

4.1 Effects of Reynolds number

Let us discuss the effects of Reynolds number on the flow around the downstream cylinder. Concerning reattachment of the separated shear layer from the upstream cylinder onto the downstream cylinder, the effects are divided into two types, (1) one accompanied with a change of its flow pattern and (2) one with its own flow pattern kept. The first type (1) appears in the range of the spacings 1.18 ≦ L/d ≦ 1.91 for Reynolds number about 2.2×10⁴. Beyond that Reynolds number, the separated shear layer reattaches onto the downstream cylinder. The second type (2) appears in the range of the spacings (a) L/d = 1.03, (b) 2.09 ≦ L/d ≦ 3.53 and (c) L/d ≧ 3.68 . The case (a) represents a flow without reattachment and the case (b) one with reattachment. The case (c) is a jumped flow beyond the critical spacing. The typical pressure distributions of the downstream cylinder in the case (1) are shown in Fig. 10 for three different Reynolds numbers. It shows that the reattachment of the separated shear layer does not occur at Re = 1.3×10⁴, but does at Re = 3.5×10⁴. The result at Re = 2.2×10⁴ corresponds to the transition region between these two patterns. Above this Reynolds number, the region of the low negative pressures on the front surface of the cylinder becomes narrow. This fact is similar to the case where the reattachment flow occurs with an increased spacing of the two cylinders. In the case of (2), the profiles of the time-averaged pressure coefficient and the R.M.S. pressure fluctuation are similar and they are independent of Reynolds number, but the magnitudes depend on Reynolds number. Let us examine the pressure coefficients C_{po} and C_{pb}, at $\phi = 0°$ and 180° respectively, which are directly related to the drag coefficient of the downstream cylinder. Both C_{po} and C_{pb} increase as Reynolds number increases. In the cases of (a) and (b) up to the critical spacing, therefore, the effect of Reynolds number on the drag coefficient is nominal, because the drag coefficient is proportional to the pressure difference ($C_{po} - C_{pb}$). On the other hand, in the case of (c) beyond the critical spacing, the drag coefficient of the downstream cylinder decreases as Reynolds number increases because the drag coefficient is dominated by the base pressure coefficient C_{pb}. This agrees with the previous results obtained by Zdravkovich and Pridden[17] and Cooper[18] .

4.2 Unstable flow and bistable flow

In the section 3.2, a hot-wire trace in the wake of the downstream cylinder in the range of the spacings 1.18 ≦ L/d ≦ 1.91 about Re = 2.2×10⁴ is very irregular. Two different values of the Strouhal number are obtained in the range of the spacings 3.09 ≦ L/d ≦ 3.53 . Let us discuss a few points on those flows.

Figures 11 and 12 show examples of the power spectrum of the velocity fluctuation and the pressure fluctuation, respectively. As shown in Fig. 11 (a) for L/d = 1.18, there exists no distinct frequency component at

NII-Electronic Library Service

$Re = 2.2\times10^4$ as pointed out by Imaichi, et al.[10] and Tokushima, et al.[11] at the Reynolds number 2.1×10^4. Let us compare the spectrum at $Re = 2.2\times10^4$ with that at lower and higher Reynolds number, i.e., $Re = 1\times10^4$ and 3×10^4 respectively. Whereas the separated shear layer from the upstream cylinder does not reattach onto the downstream cylinder at the lower Reynolds number, the shear layer reattaches at the higher Reynolds number. The spectrum at $Re = 2.2\times10^4$ is considered a superposition of those spectrums of two different flow patterns. The signal trace of pressure fluctuation as shown in Fig. 12 (a) is basically different from two traces at the spacings of $L/d = 3.09$ (Fig. 12 (b)) and $L/d = 3.53$ (Fig. 13 (b)). It shows that the flow forms one pattern momentarily, but its duration is very short and the pattern changes immediately to another pattern. This short duration flow pattern is named an unstable flow in this paper. At the spacing of $L/d = 3.09$, the existence of two different frequency components is evident beyond $Re = 1.8\times10^4$ in Fig. 11 (b). The larger frequency component is caused by the vortex shedding from the upstream cylinder. Figure 12 (b) presents the pressure fluctuation at $\phi = 90°$ on the upstream cylinder. It shows that the vortex shedding from the upstream cylinder occurs with a duration of 0.1 second to several seconds two or three times every one minite. The pressure fluctuation on the upstream cylinder is very large, but the effect of vortex shedding can be neglected for the time-averaged values. Thus, there is no effect of the vortex shedding on the pressure distribution and the R.M.S. pressure fluctuation as shown in Fig. 2 and 8 respectively. In this case, the flow is a bistable flow which has two stable flows. It can be considered that one pattern is more stable than the other. We observed a flow of the critical spacing $L/d = 3.53$, and found another type of a bistable flow. Figure 13 (a) and (b) are the flow visualization by a smoke wind tunnel and the pressure fluctuation on the downstream cylinder, respectively. It indicates that the separated shear layer from the upstream cylinder repeats reattachment onto the downstream cylinder and rolling up in front of the cylinder. And the durations of the two patterns are very long. For the bistable flow around the critical spacing, the statistical frequency of appearence and its duration of one pattern are proportional to the spacings. Figure 14 shows an example of the time-averaged pressure distribution around the downstream cylinder for the bistable flow.

4.3 Fluid flow around the cylinders

To clarify the fluid flow around the two cylinders, measurements of the pressure fluctuation on the cylinders were performed. Examples of the results are shown in Fig.15. Figures (a) and (b) are oscillograms of the downstream cylinder. The signals of the spacings of $L/d = 1.18$ and 1.91 at $\phi = 90°$ present a large fluctuation at regular intervals compared to that of the spacing of

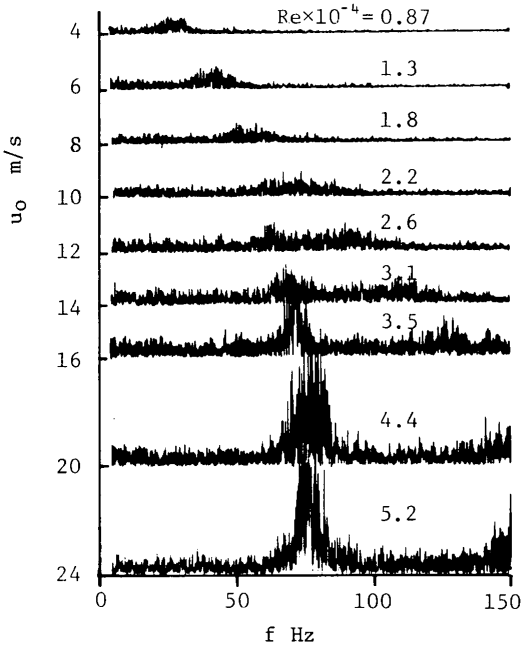

(a) $L/d = 1.18$

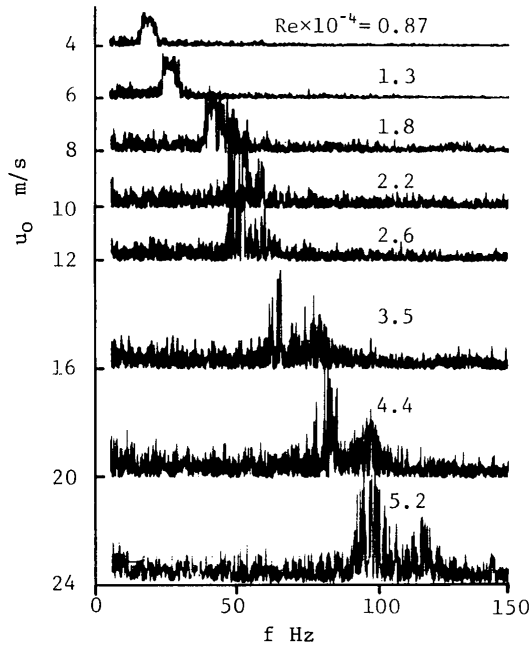

(b) $L/d = 3.09$

Fig. 11 Power spectrum of velocity fluctuation

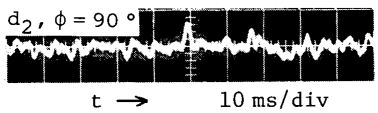

(a) $L/d = 1.18$, $Re = 2.2\times10^4$

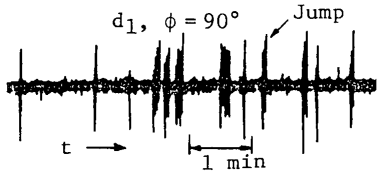

(b) $L/d = 3.09$, $Re = 3.5\times10^4$

Fig. 12 Pressure fluctuation

NII-Electronic Library Service

L/d = 1.03 without reattachment. This fact explains why the separated shear layer from both sides of the upstream cylinder are reattached alternately onto the downstream cylinder. The signal for the case of L/d = 1.18 at $\phi = 30°$ is a regular wave of which the period agrees with that of the shedding vortices. It shows a unique characteristic that the period is nearly constant irrespective of the free stream velocity as shown in Fig. 11. A detailed discussion on it is one of the subjects for a future study. This unique flow is termed a synchronized (or exciting) flow in this paper. This flow shows a similar property to that of the boundary layer suction and blowing of a circular cylinder with a two-dimensional slit placed along a diameter [19],[20]. The signal of the spacing of L/d = 1.91 at $\phi = 30°$ includes a high frequency component, which indicates the formation of quasi-stationary vortices between the cylinders. At the spacing of L/d = 2.50 as shown in the figure (b), the signals of $\phi = 0°$ and 30° show sometimes a small fluctuation, and at other times a regular large fluctuation. And the wave of $\phi = 90°$ is distorted compared with that of small spacings in the figure (a). These indicate that the quasi-stationary vortices between two cylinders are shedding intermittently. In the figure (c), the signals of both the upstream ($\phi = 90°$) and downstream cylinder ($\phi = 0°$) show a bistable flow which presents alternately a reattachment and a jump phenomenon. Figure 13 (b) is a long time record of the bistable flow.

4.4 Classification of flow patterns

The flow patterns around two circular cylinders arranged in tandem can be classified according to the longitudinal spacing between the axes of the cylinders and Reynolds number. The results and sketches of the flow patterns are shown in Figs. 16 and 17, respectively. The characteristics of the flow of those patterns are summarized as follows :

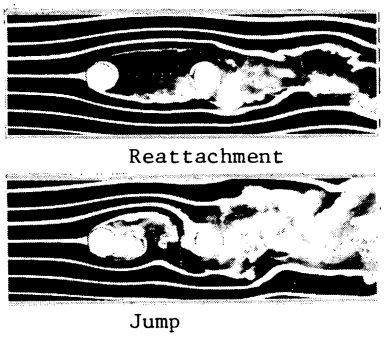

(a) Flow visualization

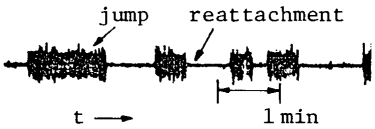

d_2 , $\phi = 0°$

(b) Pressure fluctuation

L/d = 3.53, Re = 1.3×10^4

Fig. 13 Bistable flow

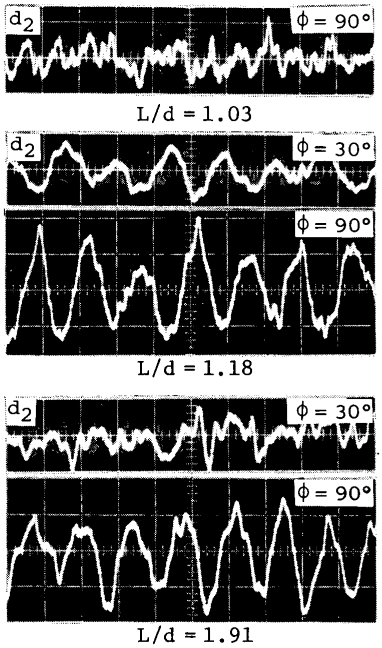

$0.4\times0.5\rho u_o^2$/div, 10 ms/div

(a) Re = 3.5×10^4

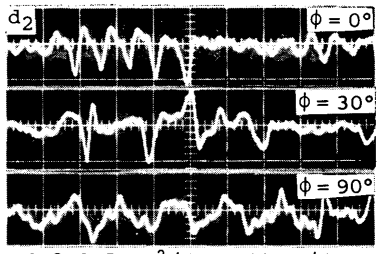

$0.8\times0.5\rho u_o^2$/div, 10 ms/div

(b) L/d = 2.50, Re = 3.5×10^4

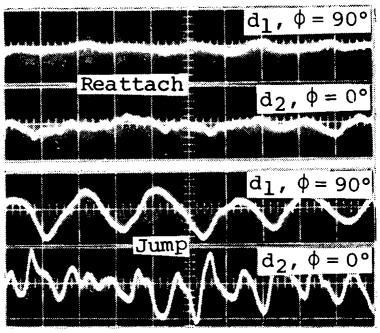

$0.5\rho u_o^2$/div, 10 ms/div

(c) L/d = 3.53, Re = 2.2×10^4

Fig. 15 Oscillograms of pressure fluctuation

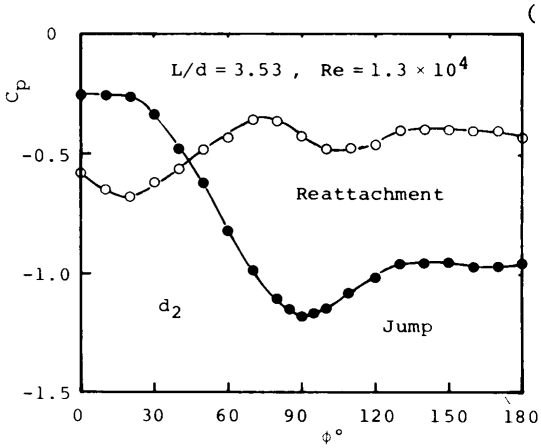

Fig. 14 Pressure distribution around downstream cylinder for bistable flow

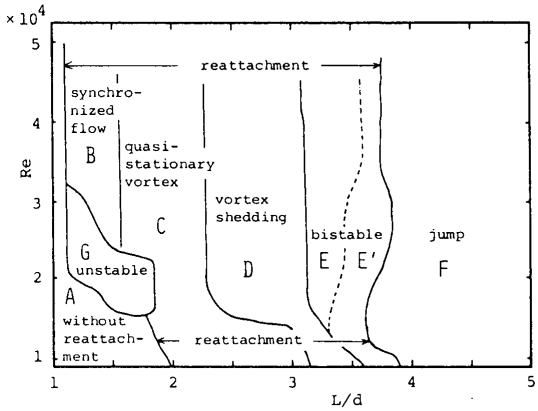

Fig. 16 Classification of flow patterns

NII-Electronic Library Service

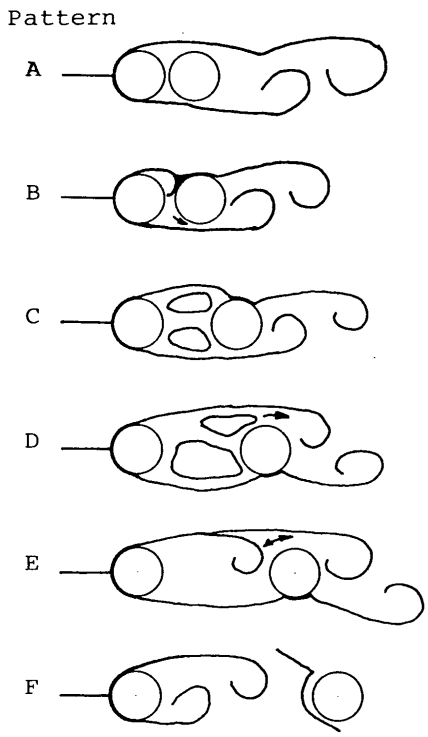

Fig. 17 Sketches of flow patterns

Pattern A : The separated shear layer from the upstream cylinder does not reattach onto the downstream cylinder.

Pattern B : Vortex formation of the shear layer and vortex shedding in the near wake of the downstream cylinder and reattachment of the other shear layer onto the downstream cylinder are synchronized. The frequency of the vortex shedding is nearly constant irrespective of the free stream velocity.

Pattern C : Quasi-stationary vortices are formed between the cylinders.

Pattern D : The quasi-stationary vortices become unstable and the vortex shedding is detected intermittently.

Pattern E : The separated shear layer from the upstream cylinder rolls up intermittently for a moment in front of the downstream cylinder. This pattern is a bistable flow in the transition region between patterns D and F.

Pattern E': A bistable flow whose one pattern continues for a long time is predominant in this region.

Pattern F : The separated shear layer from the upstream cylinder rolls up in front of the downstream cylinder.

Pattern G : This pattern is an unstable flow in the transition region between patterns A, B and C.

5. Conclusions

Experimental investigations on the characteristics of the flow around two cylinders arranged in tandem were carried out in the range of $8.7\times10^3 \leqq Re \leqq 5.2\times10^4$.

In the case where the quasi-stationary vortices are formed between the cylinders, it is found that a change of the flow structure around the cylinders takes place at a specific spacing and in a specific Reynolds number range. Classification and sketches of the flow patterns have been made. And those flow characteristics are clarified. The main results are summarized in the section 4.4.

Acknowledgements

The author wishes to thank Associate Professor T. Kamemoto of Yokohama National University and Professor H. Sakamoto of Kitami Institute of Technology for their helpful discussions. The author is also grateful to Mr. H. Uokawa, Mr. M. Kanda and Mr. M. Takahashi of National Defense Academy for their assistances in the experiments.

References

(1) Fishinden,M. and Sounders,O.A., An Introduction to Heat Transfer, Oxford Clarendon Press, (1950), p.132.
(2) Ishigai,S., et al., Bulletin of the JSME, Vol. 15, No. 86 (1972-8), p.949.
(3) Ishigai,S. and Nishikawa,H., Bulletin of the JSME, Vol. 18, No. 119 (1975-5), p. 528.
(4) Chen,Y.N., Trans. ASME, Ser. B, 90 - 1 (1968-2), P. 134.
(5) Tokushima,K., Ph. D. Thesis, Osaka University (in Japanese), (1972-12).
(6) Biermann,D. and Herrnstein,W.H.,Jr., NACA TR 468 (1933).
(7) Hori,E., Proc. 9 th Japan Nat. Congr. Appl. Mech., III - 11 (1959), p. 231.
(8) Suzuki,N., et al., Proc. Third Int. Conf. on Wind Effect on Bldgs and Structure, (1971), II - 20, p. 377.
(9) Watanabe,Y., et al., Trans. Japan Soc. Mech. Engrs. (in Japanese), Vol. 40, No. 331 (1974-3), p. 765.
(10) Imaichi,K., et al., Preprint of Japan Soc. Mech. Engrs. (in Japanese), No. 735 - 5 (1974-3), p. 104.
(11) Tokushima,K., et al., Preprint of Japan Soc. Mech. Engrs. (in Japanese) , No. 740 - 13 (1974-11), p. 13.
(12) Kostic,Z.G. and Oka,S.N., Int. J. Heat Mass Transfer, 15 - 2 (1972-2), p. 279.
(13) Hiwada,M., et al., Preprint of 15 th Annual Symp. Heat Transf. Soc. Japan (in Japanese), (1978-5), p. 10.
(14) Okajima,A., Bulletin of the JSME, Vol. 22, No. 166 (1979-3), p. 504.
(15) Igarashi,T., Preprint of Japan Soc. Mech. Engrs. (in Japanese), No. 774-13 (1977-11), p. 84.
(16) Zdravkovich,M.M., Trans. ASME, Ser. I, 99 - 4 (1977-12), p. 618.
(17) Zdravkovich,M.M. and Pridden, D.L., Journal of Industrial Aerodynamics, 2 (1977), p. 255.
(18) Cooper,K.R., National Aerodynamic Establishment, Canada, (1974), LTR - LA - 119.
(19) Igarashi,T., Bulletin of the JSME, Vol. 21 , No. 154 (1978-4), p. 656.
(20) Igarashi,T., Preprint of Japan Soc. Mech. Engrs. (in Japanese), No. 780 - 7 (1978-4), p. 101.

NII-Electronic Library Service